

SIMULATING THE FUMIGATION PROCESS USING LAGRANGIAN PARTICLE DISPERSION MODEL COMBINED WITH LARGE-EDDY SIMULATION

Si-Wan Kim, Chin-Hoh Moeng, Jeffrey C. Weil*, and Mary C. Barth

National Center for Atmospheric Research
Boulder, Colorado, USA

*CIRES, University of Colorado, Boulder, CO

1. INTRODUCTION

Fumigation is the phenomenon in which pollutants lying above the growing convective boundary layer are entrained into the boundary layer by penetrating thermal plumes. This process can increase the ground-level concentration (GLC) of pollutants significantly during daytime (e.g. Dear-dorff and Willis, 1982, hereinafter DW82). The fumigation process has been studied with Gaussian model (Meroney, 1975), water tank experiments (DW82, Hibberd and Luhar, 1996, hereinafter HL96), Lagrangian particle dispersion model (LPDM) using parameterized turbulence (Luhar and Britter, 1990), and large eddy simulation (LES) of scalar diffusion (Cai and Luhar, 2002, hereinafter CL02). In this study, the fumigation process is studied by a Lagrangian particle dispersion model driven by LES generated flows. Our objective is to check the adequacy of this new modeling approach to the fumigation process. Our results are compared with water tank experiment and Eulerian modeling of the fumigation process based on the same LES model.

2. MODEL DESCRIPTION

The LPDM adopted in this study is based on the model described in Weil et al. (2004). Particle position vector x_p at time $t+dt$ is given by

$$x_p(x_{os}, t + dt) = x_p(x_{os}, t) + u_L(x_{os}, t)dt, \quad (1)$$

where x_{os} is the initial particle position vector, t is the time, and u_L is the Lagrangian velocity vector of a particle. When using the LES flow field to drive the particles, u_L is determined by

$$u_L(x_{os}, t) = u_r[x_p(x_{os}, t), t] + u_s[x_p(x_{os}, t), t]. \quad (2)$$

Here, u_r is the resolved-scale velocity vector generated by the LES and u_s is a random subgrid-scale (SGS) velocity vector which is generated by a stochastic differential equation (see Weil et al., 2004). At the surface, a perfect reflection condition is adopted, and at the top of the mixed layer height, no constraint on particle position is applied.

For an Eulerian diffusion model, we added a conservation equation for a passive scalar in the NCAR-LES code with an area source located within or above the entrainment zone.

3. EXPERIMENTAL DESIGN

We performed two LESs, which had entrainment rates similar to those in DW82. In DW82, the dimensionless entrainment rate, w_e/w_{*0} of the slow entrainment case is 0.015 ± 0.003 , while that of the fast entrainment case is 0.042 ± 0.003 . These entrainment rates are included in the experiments of HL96 and the LESs of CL02. The stability of the free atmosphere is 0.02 K m^{-1} and 0.006 K m^{-1} for the slow and the fast entrainment rates cases, respectively. The surface heat flux is 0.05 K m s^{-1} . Initial mean wind U is set to 0 for the comparison with water tank experiments. To examine the applicability of Taylor's translation hypothesis, LES case with $Ug = 5 \text{ m s}^{-1}$ is performed separately. At the particle release time ($t = 5400 \text{ s}$), the mixed layer height z_{i0} is 260 m, convective velocity scale w_{*0} is 0.76 m s^{-1} , and eddy turnover time is 342 s.

We used the LPDM runs to investigate the effects of entrainment rate, source height (within and above the entrainment zone), and vertical depth of the initial plume on the fumigation process. Selected source heights are $z_s/z_{i0} = 1.30, 1.25, 1.19, 1.15, 1.09, 1.00,$ and 0.91 . Based on the heat flux profiles, we categorized the $z_s/z_{i0} = 1.30, 1.25, 1.19, 1.15$ as "above the entrainment zone" and $z_s/z_{i0} = 1.09, 1.00, 0.91$ as "within the entrainment zone". We examined two initial verti-

cal spread of the plume, $\sigma_{z0}/z_{i0} = 0.036$ and 0.092 , which is the same as in CL02. Eulerian model experiments based on the same LES output are designed similarly to Lagrangian model.

4. RESULTS

The definition of the height scaling parameter and the starting time of fumigation are different in the analyses of DW82, HL96, CL02. DW82 employed the time varying mixed layer height $z(t)$, HL96 used the initial plume height z_s , and CL02 used mixed layer height z_{i0} at the moment of plume insertion as a height scale. DW82 set the starting time of fumigation t_s equal to the earliest time at which the initial dye ribbon was observed to be subjected to downward diffusion motions. HL96 used t_s which is the earliest time when downward diffusion was observed to occur along a significant length of the initial fumigant ribbon. CL02 defined t_s as the plume insertion time. We define two starting time of fumigation for the our LPDM simulations. The first starting time corresponds to the time of the insertion of the plume. The second starting time is set to the time at which 5% of released particles begin to reside within the well-mixed layer below $0.85z_s$. Similar to HL96, the crosswind integrated concentrations (CWICs) are obtained from the LPDM results at $z/z_{i0} = 0.2$, and are normalized by z_s . When the starting time corresponds to the plume insertion time (Fig. 1), the near-surface CWICs clearly reach maximum values at different times, indicating a time shift with CWIC maxima for low z_s/z_{i0} occurring sooner than those with higher source heights. The modeled CWICs agree with the laboratory data for only certain heights: $z_s/z_{i0}=1.15$ for the slow entrainment case and $z_s/z_{i0}=1.15$ and 1.19 for the fast entrainment case. When the second starting time is adopted (Fig. 2), the CWICs for $z_s \geq 1.15z_{i0}$ collapse nearly to a single curve and show good agreement with the HL96 data for both slow and fast entrainment cases. In Fig.2, curves which do not collapse to the laboratory data are the ones with a plume release height within the entrainment zone. Thus, CWICs originating from source height above the entrainment zone depend on the definition of the fumigation starting time, while CWICs originating from source heights within the entrainment zone do not depend on the fumigation starting time.

The modeled CWICs near ground-level ($z_s/z_{i0} = 1.25$, $\sigma_{z0}/z_{i0} = 0.036$) are compared with those from the DW82 and HL96 experiments in Fig. 3, where the height scale in defining the

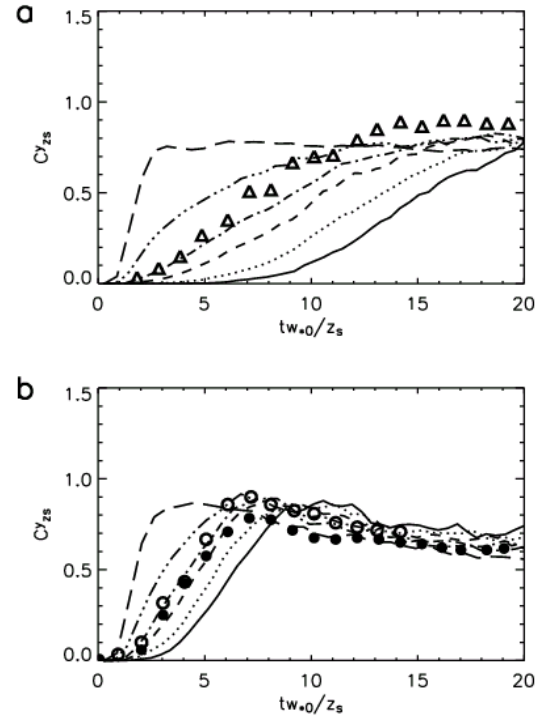


Figure 1. Dimensionless CWIC near the surface ($z/z_{i0}=0.2$) with time for (a) slow and (b) fast entrainment cases; the time origin is the plume insertion time. Solid lines represent results for $z_s/z_{i0}=1.30$, dotted lines for $z_s/z_{i0}=1.25$, dashed lines for $z_s/z_{i0}=1.19$, dash-dotted lines for $z_s/z_{i0}=1.15$, dash-triple dotted lines for $z_s/z_{i0}=1.09$, and long dashed lines for $z_s/z_{i0}=1.00$. Symbols represent the HL96 data.

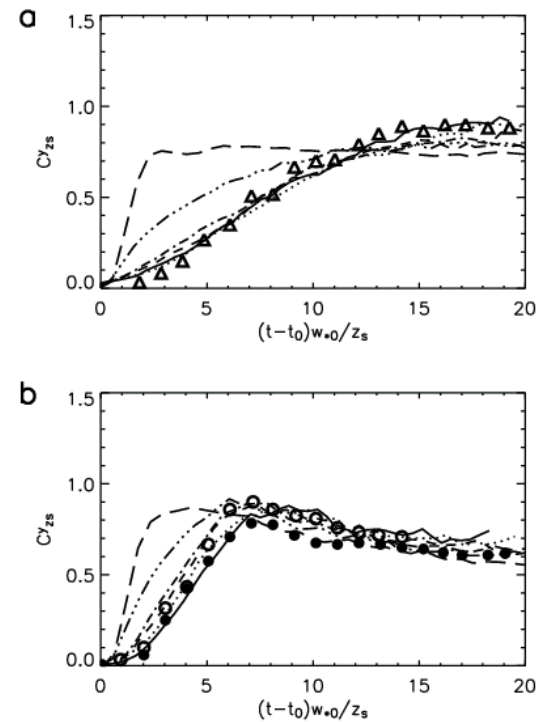


Figure 2. The same as in Fig. 1 except that the time origin is $t_0 = t_{s5\%}$.

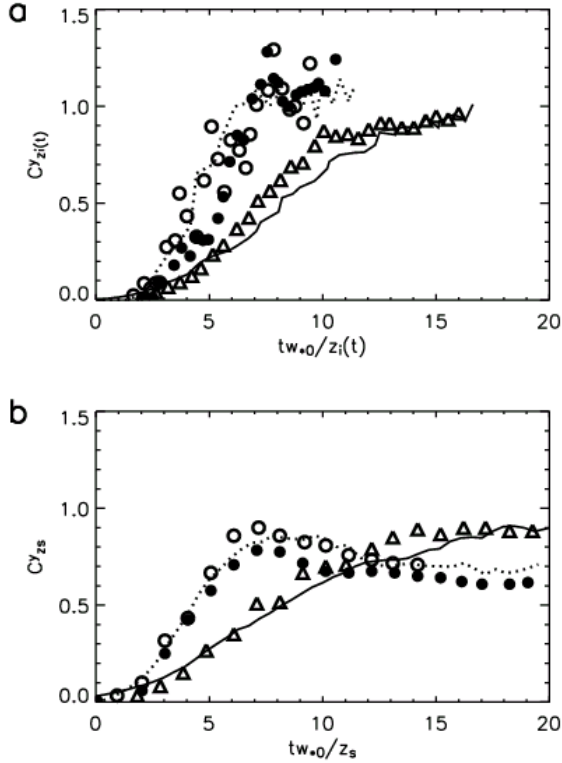


Figure 3. Near ground-level dimensionless CWICs as a function of time compared to (a) DW82, and (b) HL96. Symbols represent the laboratory data and lines the LPDM results. Filled and open circles and dotted lines apply to the fast entrainment case, the triangles and solid lines to the slow entrainment case.

dimensionless CWIC corresponds to that of DW82 ($z_i(t)$) or HL96 (z_s) and the second definition of t_s is used. Our LPDM results are quite close to both the DW82 and HL96 data.

Our LPDM results of the near surface CWICs are compared with our Eulerian diffusion model (EDM) results in Fig. 4. The EDM exhibits much greater CWIC maximum values compared to the LPDM for the releases within the entrainment zone, $z_s/z_{i0} = 0.91$ and 1.0 . This characteristic is common for both entrainment rate regimes and both cases of initial vertical spread (not shown here). For the fast entrainment case (Fig. 4b), the equilibrium (far-field) GLCs from our LPDM are greater than those from the EDM due to particle accumulation near the surface in the LPDM solution. Here, equilibrium GLCs indicate ground-level concentrations corresponding to an appropriately well-mixed vertical distribution which occurs after the completion of fumigation.

Previous studies have stated that Taylor's translation hypothesis can be applied to relation the diffusion travel time t and the downstream

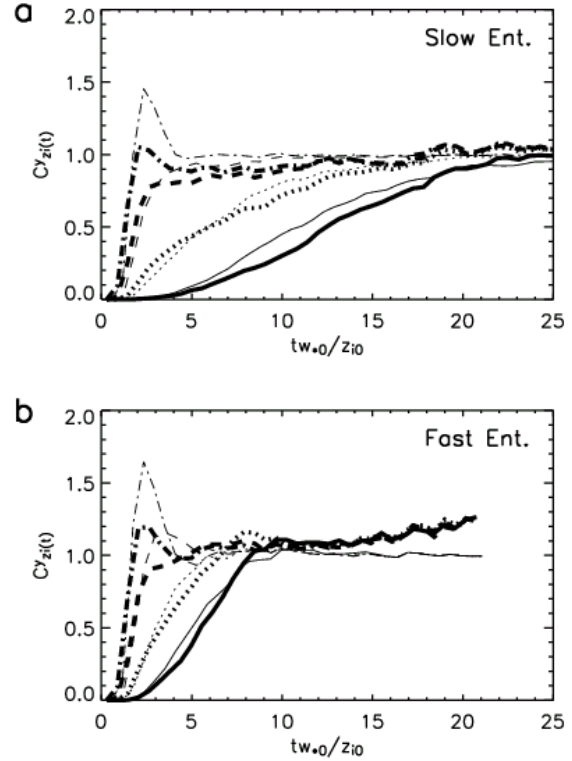


Figure 4. The dimensionless CWIC near the surface from the LPDM (thick lines) and from the Eulerian model (thin lines) with $\sigma_{z0}/z_{i0} = 0.036$ for (a) slow entrainment and (b) fast entrainment cases. Solid lines correspond to $z_s/z_{i0} = 1.19$, dotted lines to $z_s/z_{i0} = 1.09$, dashed lines to $z_s/z_{i0} = 1.0$, and dash-dotted lines to $z_s/z_{i0} = 0.91$

distance x in the fumigation process. By this hypothesis, shoreline fumigation has been regarded as the nocturnal inversion breakup fumigation, but the applicability of this hypothesis under realistic atmospheric conditions has not been proven. LES results with $U_g = 5 \text{ m s}^{-1}$ is utilized for this test. By plotting the dimensionless CWICs as a function of time and distance (Fig. 5), it is demonstrated that the CWICs calculated as a function of dimensionless time T differ from those as a function of dimensionless distance X . The GLC reaches a value of 0.1 at time 8 and 12 for T and X , respectively. CWIC difference between the two scalings also appear at dimensionless height greater than 1 because of wind shear across the entrainment zone.

5. CONCLUSIONS

This study shows that the Lagrangian modeling approach driven by LES generated flow fields is capable of reproducing results from the water tank experiments of DW82 and HL96. The near

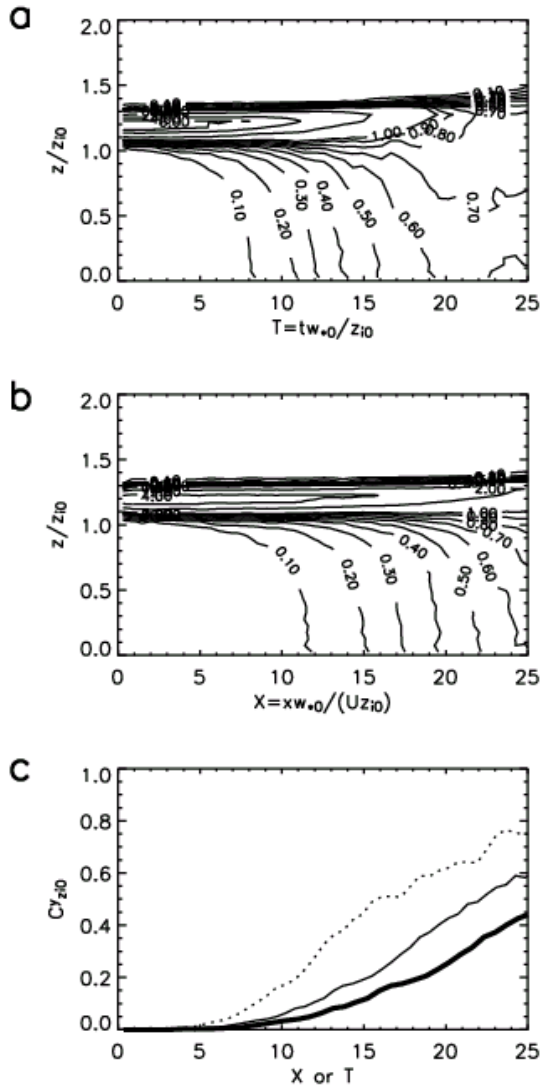


Figure 5. Dimensionless CWIC fields computed as a function of (a) dimensionless time and (b) dimensionless distance and (c) Near ground-level concentration as a function of X (thin solid, X normalized by U at the plume insertion time) and as a function of T (dotted). Thick solid line represents GLC as a function of X normalized by time averaged U . Plots are for the source height of $z_s/z_{10} = 1.19$ and plume vertical spread of $\sigma_{z0}/z_{10} = 0.036$.

surface CWIC depends on whether the initial plume height lies within the entrainment zone or above the entrainment zone. For initial plume height within the entrainment zone, some strong updrafts can reach levels within the entrainment zone, and this leads to a negligible variation of the starting time of fumigation with respect to the source height. For different initial plume heights above the entrainment zone, the near-surface

CWICs become essentially a single curve once an appropriate time shift is applied.

The differences between LPDM and EDM approaches for modeling fumigation are compared. Qualitatively both approaches based on the same LES flow field have a similar dependence of the CWICs on the entrainment rate, initial plume height, and initial plume vertical spread. However, the EDM predicts a higher overshoot of GLC than the LPDM. One aspect of the LPDM results is an undesired accumulation of particle concentration near the surface during the equilibrium state of the cast entrainment case. Further improvement to the SGS velocity model is needed for simulations of rapidly growing boundary layer.

The translation of time to distance coordinates, or Taylor's hypothesis, should be applied with caution for fumigation studies.

6. ACKNOWLEDGMENTS

The National Center for Atmospheric Research is operated by the University Corporation for Atmospheric Research under the sponsorship of the National Science Foundation.

7. REFERENCES

- Cai, X. M., and A. K. Luhar, 2002: Fumigation of pollutants in and above the entrainment zone into a growing convective boundary layer: A large-eddy simulation. *Atmos. Environ.*, **36**, 2997-3008.
- Deardorff, J. W., and G. E. Willis, 1982: Ground-level concentrations due to fumigation into an entraining mixed layer. *Atmos. Environ.*, **16**, 1159-1170.
- Hibberd, M. F., and A. K. Luhar, 1996: A laboratory study and improved PDF model of fumigation into a growing convective boundary layer. *Atmos. Environ.*, **30**, 3633-3649.
- Luhar, A. K. and R. E. Britter, 1990: An application of Lagrangian stochastic modeling to dispersion during shoreline fumigation. *Atmos. Environ.*, **24A**, 871-881.
- Meroney et al., 1975: Modelling of atmospheric transport and fumigation at shoreline site. *Bound.-Layer Meteorol.*, **9**, 69-90.
- Weil et al., 2004: On the use of large-eddy simulations in Lagrangian particle dispersion models. *J. Atmos. Sci.*, In press.